Ultra-fast, label-free isolation of circulating tumor cells from blood using spiral microfluidics

Majid Ebrahimi Warkiani[1–3,9], Bee Luan Khoo[3,4,9], Lidan Wu[5], Andy Kah Ping Tay[3,6], Ali Asgar S Bhagat[7], Jongyoon Han[3,5,8] & Chwee Teck Lim[3,4,6]

[1]School of Mechanical and Manufacturing Engineering, Australian Center for NanoMedicine, University of New South Wales, Sydney, New South Wales, Australia. [2]Medical Oncology Group, Ingham Institute for Applied Medical Research, Liverpool, New South Wales, Australia. [3]BioSystems and Micromechanics (BioSyM), Singapore-MIT Alliance for Research and Technology (SMART) Centre, Singapore, Singapore. [4]Mechanobiology Institute, National University of Singapore, Singapore, Singapore. [5]Department of Biological Engineering, Massachusetts Institute of Technology, Cambridge, Massachusetts, USA. [6]Department of Biomedical Engineering, National University of Singapore, Singapore, Singapore. [7]Clearbridge BioMedics Pte Ltd, Singapore, Singapore. [8]Department of Electrical Engineering and Computer Science, Massachusetts Institute of Technology, Cambridge, Massachusetts, USA. [9]These authors contributed equally to this work. Correspondence should be addressed to M.E.W. (m.warkiani@unsw.edu.au) or J.H. (jyhan@mit.edu) or C.T.L. (ctlim@nus.edu.sg).

Published online 17 December 2015; doi:10.1038/nprot.2016.003

Circulating tumor cells (CTCs) are rare cancer cells that are shed from primary or metastatic tumors into the peripheral blood circulation. Phenotypic and genetic characterization of these rare cells can provide important information to guide cancer staging and treatment, and thus further research into their characteristics and properties is an area of considerable interest. In this protocol, we describe detailed procedures for the production and use of a label-free spiral microfluidic device to allow size-based isolation of viable CTCs using hydrodynamic forces that are present in curvilinear microchannels. This spiral system enables us to achieve ≥85% recovery of spiked cells across multiple cancer cell lines and 99.99% depletion of white blood cells in whole blood. The described spiral microfluidic devices can be produced at an extremely low cost using standard microfabrication and soft lithography techniques (2–3 d), and they can be operated using two syringe pumps for lysed blood samples (7.5 ml in 12.5 min for a three-layered multiplexed chip). The fast processing time and the ability to collect CTCs from a large patient blood volume allows this technique to be used experimentally in a broad range of potential genomic and transcriptomic applications.

INTRODUCTION

Cancer is the second leading cause of death worldwide. The number of deaths from cancer is estimated to reach 13 million in 2030 (ref. 1). However, according to the World Health Organization (WHO), at least 30% of these deaths would be preventable if patients are diagnosed and treated before the occurrence of cancer metastases, as the metastases are believed to cause ~90% of cancer-related deaths[2]. Cancer metastases arise after the dissemination of CTCs into the peripheral bloodstream from primary or secondary tumor sites[3,4]. CTCs were first discovered in 1869 by Ashworth[5], but their significance in cancer biology has only emerged recently[6]. This delay is largely attributed to the difficulty in reliable CTC detection and isolation, as CTCs are ultra-rare, with an occurrence frequency of ~1 in ~10^7 leukocytes in the peripheral blood of cancer patients[7]. In the past 10 years, the use of CTCs as a real-time liquid biopsy has received much attention, and further analysis of these cells may greatly advance our understanding of the metastatic cascade, tumor evolution, heterogeneity and resistance to therapy[8]. Hence, there is great incentive for a robust cell separation technique that allows fast and efficient isolation of CTCs for downstream analysis.

Existing approaches for CTC isolation

In 2004, the CellSearch System (Janssen Diagnostics) was approved by the US Food and Drug Administration (FDA) for CTC isolation and enumeration. Despite CellSearch's limitations in methodology, physics, statistics and inter-operator variability, no other similar medical instrument has been clinically approved for market entry in the past decade. Other means of CTC detection are available, but they are mostly restricted to the bench, with limited capacity to process large blood volume[8,9]. Bulk blood processing equipment, such as flow cytometers and fluorescence scanning microscopy, have also been used for CTC isolation. Although these techniques require simple and readily available tools for operation, they are known to lose rare cells and to compromise viability[10]. Conventional size-based filtration, such as the method termed as 'Isolation by Size of Epithelial Tumor cells (ISET)', has also been used to isolate CTCs, using the advantage of size differences between cancer cells and blood cells[11,12]. However, despite the ease and low cost of operation, issues related to filter clogging and high degree of damage to isolated cells still arise.

Microfluidics approach. The advancement of technology in the field of microfluidics has led to the rapid development of various devices to improve the separation efficiency and recovery rate of the CTC isolation process. Unlike conventional techniques, these miniaturized systems offer advantages, such as higher sensitivity, purity, lower cost and compatibility with downstream assays or total analysis systems[13,14]. One of the most common approaches to CTC isolation is to use antibody-antigen interactions. A diverse range of magnetophoretic separation systems have been developed over the past decade for CTC isolation. A core advantage of magnetophoretic separation over the CellSearch platform is its continuous operation and higher throughput. Moreover, the miniaturized systems enable precise manipulation of cells and force field at the micrometer scale, and thus they have been shown to achieve better performance in antibody-based CTC isolation as compared with their macroscale counterparts. For example, IsoFlux, a newly developed microfluidic platform by Fluxion Biosciences, uses microfluidic channels to ensure sufficient and reliable exposure of magnetic particle–tagged CTCs to intensive and highly uniform magnetic fields for efficient cell recovery[15]. There are also a diverse range of microfluidic systems with geometrically enhanced microstructures (microposts), which improve the CTC capture efficiency by

increasing collision frequency between target cells to antibody-coated substrate, including the CTC chip developed by Nagrath *et al.*[16] and the geometrically enhanced differential immunocapture chip developed by Kirby and colleagues[17].

Affinity-binding approaches (label-dependent). Nanostructures, such as silicon nanowires, nanoclusters and nanobeads, have also emerged as promising CTC detection platforms[18,19]. CTCs are enriched by combining the preferential adhesion of cancer cells to nanostructured surfaces with conventional antibody-based affinity interactions. One major challenge in using those affinity-based cell enrichment techniques is the heterogeneity in biomarker expression of CTCs[20], including the decreased surface expression of the common capture target, EpCAM, during the process of epithelial-mesenchymal transition (EMT)[21]. Carcinoma cell lines derived from the same tumor type (for example MCF-7 and MDA-MB-231) can have different surface density for EpCAM binding (222.1×10^3 and 1.7×10^3, respectively)[22]. In light of this problem, teams are starting to explore other organ- or tumor-specific markers such as EGFR[23], HER-2 (ref. 24) and MUC-1 (refs. 25,26), and to use antibody cocktails for CTC capture[27]. Another issue regarding the specificity of CTC isolation is the possibility of entrapping leukocytes expressing similar epithelial markers[28]. Mature erythrocytes possess distinct biological or physical properties that allow them to be removed from the blood easily through gradient centrifugation and lysis[29,30]. However, some leukocytes may share similar properties with CTCs, and they can persist within the enriched sample compromising the purity of isolated CTCs. To overcome these limitations, methods that negatively deplete blood cells[31] such as EPISPOT[32] (CHU and UKE) or ^{neg}CTC-iChip (MGH)[33] have been demonstrated to isolate CTCs in an unbiased way. In most of the negative-selection techniques, leukocytes are usually removed via fluorescent or magnetic beads coated with CD45-specific antibody[34]. Nevertheless, any biochemical means of enriching CTCs or depleting other blood cells may either potentially lose CTCs because of heterogeneous biomarker expression or result in inefficient removal of unwanted cells because of compromised sensitivity and specificity. Antibody binding may also induce cytotoxicity[35], which is detrimental for downstream assays investigating CTC biology. In light of cancer heterogeneity and the importance of single-cell analysis, the loss of any CTCs because of nonspecific binding to antibody-coated magnetic beads may result in an incomplete identification of isolation of CTCs, thereby limiting a full understanding of their biology[36].

Label-free approaches. The persistent challenges faced by users of affinity-binding techniques has encouraged the development of label-free microfluidic CTC isolation techniques based on biophysical characteristics such as size[37–39], density[40], deformability[41] or dielectric properties[42,43]. However, many of these label-free microfluidic approaches suffer from low throughput[44] and other drawbacks such as clogging, low recovery, complicated integration of external force fields and possible loss of cell viability, which hinder their prevalent use, especially in clinical settings[2]. Current techniques in development are attempting to overcome some of these issues. These developments enable the isolation of viable CTCs, which has led to the reported development of certain cell lines[45], albeit of low efficiency. One example is the Vortex chip[46] that makes use of deformability and size differences between cancer cells and blood cells for CTC enrichment. The ease of fabrication and low cost, coupled with high white blood cell (WBC) depletion, makes it an attractive alternative for CTC enrichment. However, similarly to many other techniques, the Vortex chip is limited by its sample processing speed. Furthermore, size-based enrichment techniques are often unable to recover smaller CTCs. Karabacak *et al.*[47] combined the techniques of deterministic lateral displacement, inertial focusing and magnetic beads to achieve 3.8-log depletion of WBCs for CTC enrichment. However, the use of two separate modules currently necessitates additional production processes. To overcome these limitations, researchers capitalize on the differences in membrane electric properties (dielectrophoresis) to isolate CTCs[42,43]. Such devices are more sensitive, but they are costly and difficult to manufacture.

Our team has recently developed an ultra-high-throughput size-based separation method for CTC separation, isolation and retrieval from blood[48]. Our technology can achieve up to 4-log WBC depletion using a much simpler fabrication protocol and with higher throughput. This method takes advantage of the distinct focusing positions of larger CTCs apart from the smaller blood cells as a consequence of combined inertial and Dean drag forces in a spiral microfluidic device, enabling rapid and continuous isolation of viable CTCs (**Fig. 1**). The simplicity and robustness in device operation, along with its high throughput, ensures the feasibility of using our CTC separation method in a clinical setting. As a result, the technique presents few technical limitations and demonstrates high recovery, viability and WBC depletion (**Supplementary Table 1**).

By using this device, we successfully demonstrated CTC isolation and detection in blood samples of patients with metastatic

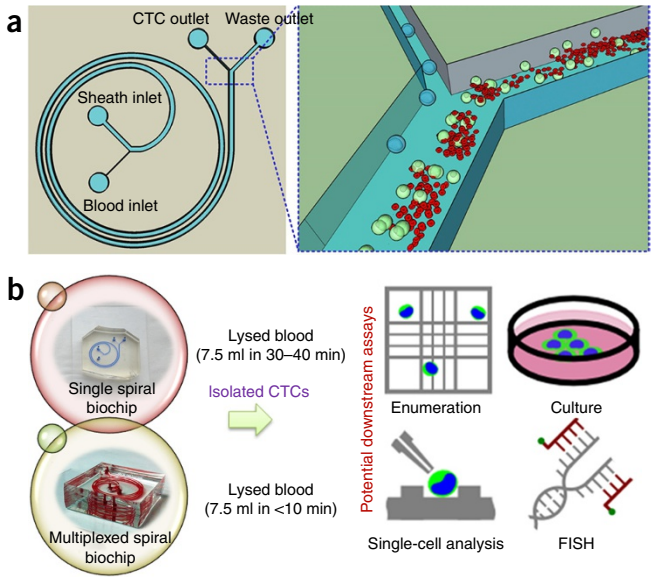

Figure 1 | Overview of CTC isolation using spiral microfluidics. (**a**) Schematic of CTC enrichment by a spiral channel. CTCs are focused near the inner wall, whereas WBCs, RBCs and platelets are focused closer to the outer wall at the outlet because of the combined effects of inertial lift force and Dean drag force. (**b**) Left, optical image of single and multiplexed spiral biochips for high-throughput CTC isolation from lysed blood. Right, schematic illustrating the possible downstream techniques for functional characterization of CTCs isolated using a spiral biochip.

lung and breast cancer, with close to 100% detection sensitivity[48]. The device is capable of handling large volumes of blood (compared to any existing microfluidics system), and it offers continuous collection of viable CTCs, which facilitates subsequent *in vitro* CTC culture. Furthermore, a crucial advantage of this chip is the potential ability to return all fractions of blood required for biomarker studies—plasma, CTCs and peripheral blood mononucleated cells (PBMCs)[49]. For this device, ~10s to 10,000s of WBCs per ml of blood (median from 30 samples = 3,109 WBCs per ml) remain after spiral chip processing, but the purity of enriched CTC samples is sufficient for downstream sequencing or fluorescence *in situ* hybridization (FISH) analysis, as demonstrated here and in previous papers[49,50]. Thus, the benefit of isolating more CTCs arguably outweighs the presence of WBC contamination.

Development of the protocol

Key requirements of a rare-cell separation technique include the following: (i) high separation resolution, (ii) high purity of separated cells, (iii) high throughput to process larger sample volumes, (iv) versatility to adapt to different cell types and (v) operational robustness. Microfluidic cell separation devices offer distinct advantages over traditional cell sorters, for example, portability, which facilitates the development of point-of-care diagnosis, and higher separation resolution, because channel dimensions are optimized to cell size to allow better control over separation. The spiral microchannel for CTC isolation was developed to meet these requirements.

Principle of operation. Lateral migration of particles because of inertial forces was first shown by Segre and Silberberg[51,52] in the 1960s when it was observed that randomly dispersed ~1-mm-diameter particles formed an annulus in a 1-cm-diameter pipe. Since then, various researchers have conducted experimental work to understand this phenomenon. Karnis *et al.*[53] observed that at larger flow rates particles focused closer to the wall. Larger particles also stabilize nearer to the center of the channel because of inertia effect of flow (**Fig. 2a**). Tachibana[54] also found that the ratio of the sphere diameter to the channel diameter affects the lateral migration of spheres in pipe flow. These observations have been validated with the advent of microfluidics technology[13,55]. Later, Di Carlo[56] and other groups[57] showed that the addition of curvatures introduced secondary cross-sectional flow field perpendicular to the primary flow direction (Dean flow)[58]. Therefore, particles in a spiral channel can migrate across main streamlines by following secondary vortex. As channel dimension affects the equilibrium positions of particles and cells[59], it is possible to design the spiral channel to enable the focusing of only the larger target particles and cells near the inner wall while leaving the smaller unwanted particles and cells dispersed and following the streamlines. As a result, one could appropriately achieve a situation at the channel outlet region, whereby larger particles are focused and aligned near the inner wall, whereas the smaller particles occupy the lateral position near the outer wall. Taking advantage of this phenomenon, we designed the spiral microchannel with appropriate dimension for separation between larger CTCs and smaller blood cells (**Fig. 2b**). The microchannel design parameters can be easily adjusted using our analytical model described below to change the size cutoff (the size above which the particles and cells are focused and below which they are not).

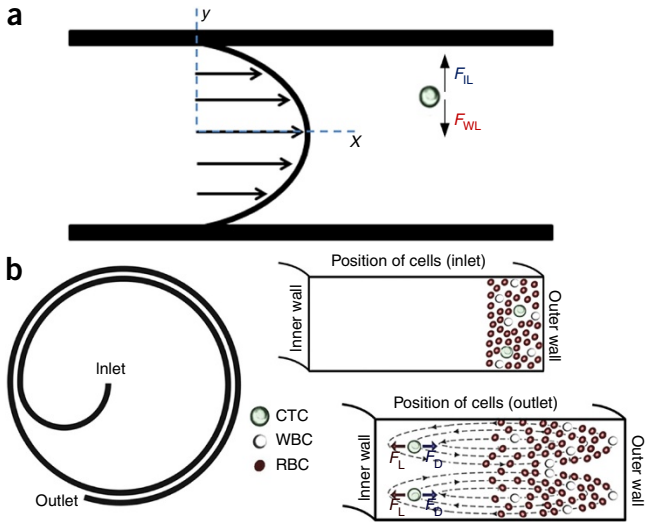

Figure 2 | Schematic illustration and working principle of particle or cell focusing in straight and curvilinear microchannels. (**a**) Particles in a rectangular straight channel experience hydrodynamic forces, namely shear-induced lift force (F_{IL}) and wall-induced lift force (F_{WL}), causing them to focus along the channel perimeter. (**b**) Operating principle of CTC enrichment by a spiral channel with rectangular cross-section. Blood sample is pumped into the outer inlet of the device while sheath fluid is passed through the inner inlet. CTCs are focused near the inner wall because of the balance of inertial lift force (F_L) and Dean drag force (F_D) at the outlet, while hematologic cells (RBCs, WBCs and platelets) migrate along the Dean vortices, exiting the device from the outer outlet.

In a curvilinear microchannel, the magnitude of Dean vortices is quantified by a nondimensional parameter Dean number (De) (ref. 57) given by

$$\mathrm{De} = \frac{\rho U_F D_H}{\mu}\sqrt{\frac{D_H}{2R_C}} = \mathrm{Re}\sqrt{\frac{D_H}{2R_C}} \quad (1)$$

where ρ is the fluid density, U_F is the average flow velocity, μ is the viscosity of the fluid, R_C is the radius of curvature of the path of the channel, D_H is the channel hydraulic diameter and Re is the flow Reynolds number (ratio of inertial to viscous force). These Dean flows generate a drag force on the particles and cells entraining and driving them along the direction of flow within the vortices. This motion translates to the particles moving back and forth across the channel width between the inner and outer walls with increasing downstream distance when visualized from the top or bottom. The velocity with which these cells migrate laterally when flowing in a channel is dependent on the Dean number, and it can be calculated as follows:

$$U_{\mathrm{Dean}} = 1.8 \times 10^{-4} De^{1.63} \quad (2)$$

The lateral distance traversed by a particle along the Dean vortex can be defined in terms of 'Dean cycle'. For example, a particle that is initially positioned near the microchannel outer wall and then migrates to the channel inner wall at a given distance downstream is said to have completed half a Dean cycle. The same particle then migrates back to the outer wall, and it is said to complete 1 Dean cycle. For a given microchannel length, the particles can thus undergo multiple Dean cycle migration with

increasing flow rate (Re) conditions. The length for 1 Dean cycle migration can be calculated as follows:

$$L_{DC} \approx 2w + h \quad (3)$$

where w is the microchannel width and h is the microchannel height. Consequently, the total microchannel length required for Dean migration is given by

$$L_C = \frac{U_f}{U_{Dean}} L_{DC} \quad (4)$$

The magnitude of Dean drag force is given by Stokes' law:

$$F_D = 3\pi\mu U_{Dean} a_c \quad (5)$$

where a_c is the cell diameter.

Apart from the Dean drag force, larger particles with a diameter comparable to the microchannel dimensions also experience appreciable inertial lift forces (F_L) (both shear and wall-induced), resulting in their focusing and equilibration. The parabolic velocity profile in Poiseuille flow results in a shear-induced inertial lift force acting on the particles, which directs them away from the microchannel center toward the channel walls. As these particles move closer to the channel wall, the abrupt presence of the wall disrupts the rotational wake formed around the particles, inducing a lift force and thus directing them away from the wall toward the microchannel center. As a result of these two opposing lift forces, the particles equilibrate (focus) around the microchannel periphery at distinct and predictable positions. This effect is dominant for particles with a size comparable to microchannel dimensions $a_c/h > 0.07$. The magnitude of F_L is given by

$$F_L = C_L \rho G^2 a_c^4 \quad (6)$$

where C_L is the lift coefficient, which is a function of the particle position across the channel cross-section assuming an average value of 0.5, and G is the shear rate of the fluid. The average value of G for a Poiseuille flow is given by $G = U_{max}/D_H$, where U_{max} is the maximum fluid velocity and can be approximated as $2 \times U_F$.

$$F_L = \frac{2\rho U_F^2 a_c^4}{D_H^2} \quad (7)$$

In microchannels with curvilinear geometry, the interplay between the inertial lift force (F_L) and the Dean drag force (F_D) reduces the equilibrium positions to just two near the inner channel wall, each within the top and bottom Dean vortex. The two equilibrium positions overlay each other along the microchannel height, and they are located at the same distance from the microchannel inner wall for a given particle size—i.e., viewed as a single position across the microchannel width. By taking advantage of these two phenomena—i.e., Dean migration and inertial focusing—we can now separate particles and cell mixtures of varying sizes. As an application of this new technology, we demonstrated its ability for cancer cell isolation from blood. CTCs are extremely rare in blood, comprising as few as one cell per 10^7–10^9 hematological cells per milliliters in patients with metastatic cancer[60]. Hence, isolation and enumeration of CTCs has been a huge technical challenge. The spiral biochip exploits the size difference between the CTCs, which are typically ~15–20 μm in diameter, and the other blood cells (red blood cells (RBCs) and platelets ~3–8 μm; WBCs ~10–15 μm) for cell separation.

Design of spiral biochips. As a starting point for the development of our method, we used a simple two-inlet, two-outlet spiral to directly isolate CTCs from lysed blood. As described in the operation principle, the primary design factor of a working spiral cell sorter is to have a microfluidic channel with appropriate channel depth that allows the inertial focusing of only large target cells near the inner wall while leaving the rest of the smaller untargeted cells dispersed and following the streamline away from the inner wall. Previous optimization works done to investigate bead behavior in spiral channels (500 μm in width, ~1 cm in radius of curvature) demonstrated that particles achieved tight focusing along the inner wall when satisfying $a_c/h \sim 0.1$ (ref. 61). Thus, for separation between CTCs (≥15 μm) and blood cells, including RBCs, platelets and WBCs (~3–15 μm), a working spiral CTC isolator should have a channel depth of ~150–180 μm. We then determined the channel length of the CTC isolator on the basis of equation (4) under a Reynolds number of ~20–100, at which the inertial focusing of large particles usually occurred. We designed the inlet split of CTC isolator to be 75 μm for sample inlet near the outer wall and 425 μm for sheath inlet near the inner wall so that the small width of sample inlet forces all the cells entering the spiral channel and beginning their lateral migration at a similar position. The split design of the channel outlet was determined by studying the lateral location of particles and cells across channel width under different flow rates. Briefly, we first identified the flow rate range required for large 15-μm-diameter particles (representing CTCs) to focus near the inner wall and the combined sets of flow rate and channel length required for small 6-μm-diameter particles (representing RBCs) to travel one complete dean cycle, respectively. Under the flow rate and channel length window satisfying both requirements, we measured the distribution of particles across the channel width under different input cell concentrations and identified the optimal position of outlet split to be 150 μm wide for CTC collection outlet near the inner wall and 350 μm wide for waste outlet near the outer wall[48].

Initially, we designed our spiral system (i.e., two-stage cascaded system) for the isolation of CTCs from whole blood[48]. We have shown that the cascaded spiral biochip is capable of processing blood with hematocrit of 20–25%, thus allowing processing and enrichment of rare cells with ~3 ml/h speed (7.5 ml in 150 min). However, to substantially increase the throughput of our system while simplifying operation and also automation, we modified our protocol to include an RBC lysis step for improved yield and target cell purity. Nucleated cells resulting from RBC lysis were resuspended in saline to 0.5× of original whole blood volume (2× concentrated, ~14×10^6 nucleated cells per ml) before the spiral processing. This RBC lysis pretreatment step substantially reduces the amount of untargeted blood cells in the sample and thus mitigates the undesired cell dispersion due to cell-cell interaction (7.5 ml in 37.5 min for single chip). In addition, we further improved the throughput of spiral cell sorting by stacking

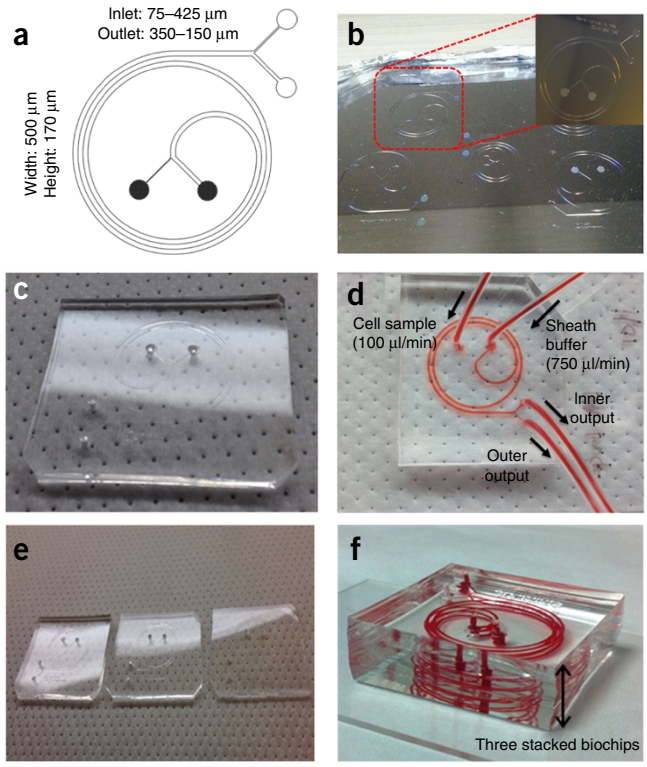

Figure 3 | Illustration of different steps for fabrication of spiral microfluidic chips. (**a**) CAD drawing, (**b**) fabrication of the mold using standard microfabrication techniques. (**c**) Soft lithography and pattern transfer to a single layer of PDMS using the fabricated mold. The fluidic access for inlets and outlets is pierced into the device using precision punches. (**d**) A completed spiral device after bonding to a glass slide. Red food coloring was used for better visualization of the channels. (**e**) Three individual PDMS replicas with pierced fluidic access. (**f**) A multiplexed spiral biochip obtained by stacking three individual biochips together using plasma bonding and manual alignment.

three spiral CTC cell sorters together to build a multiplexed system. The 3× multiplexed system has common inlets and outlets for the three spiral sorters working in parallel with each other[49]. The 3× multiplexed system operates at a much higher throughput, thus it facilitating the processing of larger blood volumes (7.5 ml in 12.5 min for multiplexed chip).

Experimental design

Device fabrication and multiplexing. The device design consists of a two-loop spiral microchannel with two inlets and two outlets with a radius of ~10 mm. The width of the channel cross-section is 500 µm, and the outlet bifurcation is optimized to be 150–350 µm (**Fig. 3a**).

We use standard microfabrication techniques to fabricate the silicon master of microfluidic channels and to produce spiral microchips (Steps 1–8), as described previously[62]. Briefly, 6-inch-diameter silicon wafers are first patterned using standard UV lithography and etched using deep reactive-ion etching (DRIE) to define the channels on the wafer (~170 µm etch depth). After etching, the patterned silicon wafers (**Fig. 3b**) are cleaned using acetone and isopropanol and treated with trichloro (1*H*,1*H*,2*H*,2*H*-perfluorooctyl) silane for 2 h to facilitate polydimethylsiloxane (PDMS) mold release. After silanization, PDMS prepolymer is mixed in a 10:1 (wt/wt) ratio with a curing agent and poured onto the silanized wafer. The wafer is baked at 80 °C for 1–2 h. After curing, the PDMS is peeled from the mold, and access holes (1.5 mm) for fluidic inlet and outlets are punched (**Fig. 3c**). We use a Uni-Core puncher (Sigma-Aldrich), and we irreversibly bond the PDMS devices to microscopic glass slides using an oxygen plasma machine to complete the channels (**Fig. 3d**). To fabricate a multiplexed device, three PDMS molds are fabricated (**Fig. 3e**) as described above and stacked together using plasma bonding and manual alignment (Step 19). The final device is irreversibly bonded to a glass slide using the oxygen plasma machine, and it is placed inside an oven at 70 °C for 30 min to further enhance the bonding (**Fig. 3f**). The chip is then primed (Step 20) ready for use (Steps 20–26).

Characterization using surrogate microbeads and cell lines. An important aspect of the device optimization process is to characterize the behavior of particles or cells under flow within the designed cell sorter. As described previously, the optimal channel depth and outlet split design, as well as operational flow rates, were eventually determined on the basis of actual experimental results. To save cost and time, initial device characterization was usually done with surrogate particles, as proposed in Step 27 of the PROCEDURE. To mimic components of blood, we used particles with diameters of 6, 10 and 15 µm, representing RBCs, WBCs and CTCs, respectively. We also performed a confirmatory check with actual cancer cell lines on the newly synthesized optimized system to validate results generated from particle studies (**Fig. 4a**). Device characterization with cell samples is ideal for identifying any discrepancy in the hydrodynamic behavior between the rigid microbeads and deformable cancer cells. We achieve this by flowing lysed blood (WBCs) or cancer cells from cell lines, separately, into the optimized device and observing the distribution of the cells across channel width at outlet region (**Fig. 4b**). A microscope equipped with a phase-contrast light source and a high-speed camera is used. Overall, the channel dimensions optimized on the basis of particle result should work well with an actual cell sample; however, the optimal operational flow rate will be slightly different, as the interaction between fluid and deformable cells introduces additional lift force. This additional force affects the exact equilibrium position of cells within the channel cross-section. We have observed the distribution of particles or cells across channel widths at different positions along the channel length under various flow rates.

For consistency, we fixed the sample input flow rate as 100 µl/min and varied the sheath buffer flow rate to study the effect of total flow rate on particle and cell behavior. For larger (>15 µm) particles and cells, we primarily looked at the outlet region of the spiral channel, as larger particles and cells did not move much in lateral direction once they reached their equilibrium positions near the inner wall. For the smaller particles and cells, we monitored their behavior along the channel length, mediated by lateral Dean migration. Optimally, the smaller particles and cells should move from the side of the outer wall at the inlet region to the side of the inner wall first, and then back to the region nearer to the outer wall with some dispersion (i.e, undergo a complete Dean cycle) as they travel along the channel length. Adjustment of the sheath buffer flow rate (and thus total flow rate) could change the number of Dean cycles that the small particles and cells undergo within a channel of a given length.

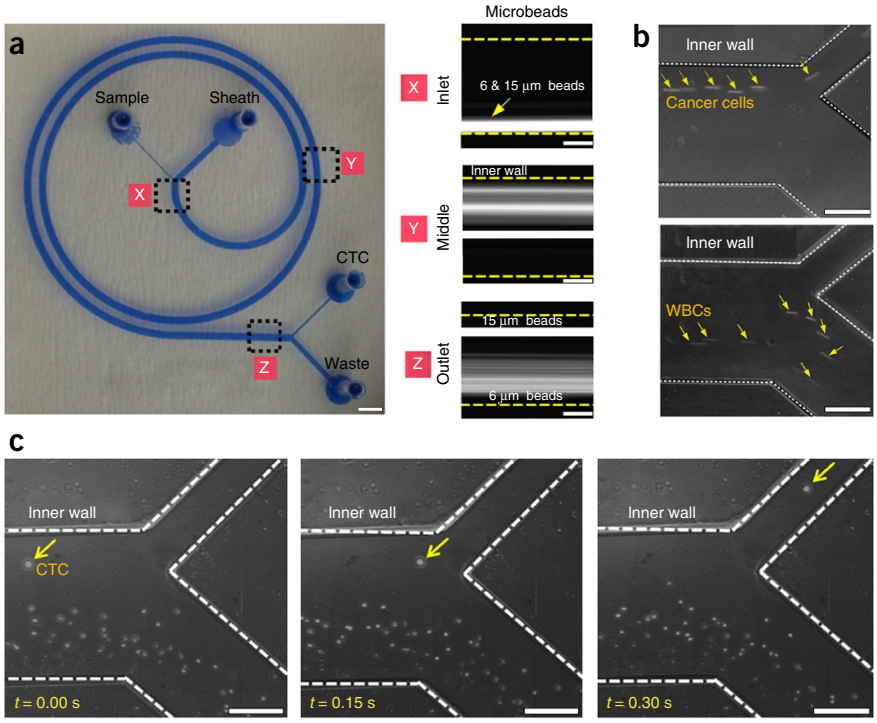

Figure 4 | Characterization of the spiral biochips for CTC isolation. (**a**) Left, a photograph of the spiral device developed for isolation of CTCs (the microchannel is filled with a blue dye for visualization). Scale bar, 2 cm. Right, validation of the design principle using fluorescently labeled polystyrene particles. Superimposed images illustrating distribution and position of the 6- and 15-µm particles at the inlet (X), in the middle of the channels (Y), and at the outlet (Z). The randomly distributed particles at the inlet form ordered focused streams, which are then collected separately at outlets. Scale bars, 50 µm. (**b**) Top, average composite images representing the focusing position of MCF-7 cells at the outlet of the spiral device. Bottom, average composite images representing the focusing position of WBCs at the outlet of the spiral device. Scale bars, 200 µm. (**c**) Time sequence images demonstrating the isolation of CTCs from lysed blood using a spiral microfluidic biochip. Dashed lines mark the border of the microfluidic channels in all panels. Scale bars, 200 µm.

Isolation of spiked cell lines from lysed blood samples. In actual samples, CTCs are present at low frequencies with blood cells, including RBCs (billions per ml whole blood), platelets (millions per ml whole blood) and WBCs (millions per ml whole blood), which in total constitute ~99.99% of the cell counts in a clinical whole blood sample. The presence of blood cells, along with the target cancer cells, will affect cell focusing and flow within the spiral channel. To reduce the amount of cellular components flowing in the spiral biochip, we use a conventional RBC lysis technique (using ammonium chloride solution) in order to boost the throughput (Steps 28–31). Although WBCs constitute only 1% of the total blood volume fraction, it is still challenging to separate CTCs from them efficiently. Extensive characterization of the proposed methodology was carried out to study the depletion capability of WBCs in the spiral biochip[49,62]. Removal of most of the RBCs via lysis enables us to process the sample without dilution (increasing throughput), and it enables better separation of the larger cancer cells from the smaller blood cells (due to reduced cell concentration; **Fig. 4c**). Moreover, we have shown that this additional pre-processing step does not compromise cancer cell recovery, and it also does not alter the viability and morphology of the recovered cells.

To test the performance of the spiral biochip for CTC isolation and recovery, we characterized the biochip with commercially available cancer cell lines (**Supplementary Videos 1–3**). Different cell lines were used as they exhibited a varied range of cell sizes, which enabled the device to be optimized for the isolation of CTCs of different cancer types (**Supplementary Fig. 1** and **Supplementary Table 2**). We demonstrated the successful sorting of spiked cancer cells from blood components with high degree of recovery (~85%) across multiple cell lines for clinically relevant spiking doses. Purity of the enriched sample is very important for many downstream molecular assays in which the contaminating materials from WBCs can substantially lower the signal to noise leading to inaccurate diagnosis. Starting with an initial concentration of ~14×10^6 nucleated cells (7.5 ml of blood is lysed and resuspended into 3.75 ml of PBS) the spiral biochip can deplete ~ 99.99% of the WBCs from healthy samples, thus providing a purer CTC fraction at the outlet. However, the capture purity for clinical samples is a function of multiple variables, such as the number of isolated CTCs and also the number of contaminated WBCs (which normally vary from one patient to another one depending on the type of cancer), quality of blood (i.e., some patients show high number of WBCs in their blood due to the chemotherapy), cancer stage and so on. Therefore, talking about sample purity is subjective, and it can change from one sample to another. **Supplementary Table 3** shows some of our recovered cell counts obtained from patients with breast or lung cancer.

Applications of the protocol

The spiral chip can be useful for both research and clinical applications. CTC quantification may offer insight on cancer progression, treatment efficacy and survival prognosis. Cristofanilli *et al.*[63] first showed in their landmark study that patients characterized with five CTCs per 7.5 ml of peripheral blood had poorer overall survival. The therapy study conducted by Hayes and co-workers[64] also supported the prognostic properties of CTCs. Therefore, CTC enumeration can have paramount clinical significance to guide decisions in personalized treatments.

CTC can also be an asset for research to shed greater light on cancer biology. CTC interrogation can be performed using DNA- or RNA-FISH (**Box 1**) or genetic analytical techniques[50]. The immunoproperties of CTCs from different cancer stages, types and locations may reveal important differences related to diagnostics[65,66]. CTC cultures[67–69] can also be used for drug testing in various platforms such as 3D microfluidics systems[70]. Recently, there has been increased interest in studying the cancer genome. By performing genome sequencing and mapping of enumerated CTCs, DNA or RNA regions common to malignant cancer may be identified, thus facilitating drug discovery.

Box 1 | DNA-FISH ● TIMING 2 d

As an alternative to Steps 38–47 of the main PROCEDURE, CTCs can be characterized by DNA-FISH, as described below.

Additional materials required for FISH

RNase (Sigma-Aldrich, cat. no. R6418).

FISH probes of interest: for example, we used Vysis *ALK* break-apart FISH probe and HER2/*neu* (Abbott Laboratories) probe to obtain the results shown in **Figure 6**.

Fixation

1. Concentrate the samples collected in Step 37 by centrifugation at 300*g* for 3 min at room temperature.
2. Resuspend the cell pellet gently in acetic acid/methanol in a 1:3 ratio to fix cells.

■ **PAUSE POINT** Fixed cells can be stored at –20 °C for 2–3 weeks until use.

Hybridization

3. Add acetic acid/methanol-fixed cells dropwise onto slides, and treat the cell spot with RNase (4 mg/ml) for 40 min at 37 °C.

▲ **CRITICAL STEP** Slides with cells should be freshly prepared for FISH procedures.

4. Wash cell spots in 0.2% (vol/vol) Tween 20 in PBS.
5. Denature the cell spots with 70% (vol/vol) formamide/2× SCC for 10 min at 80 °C.
6. Dehydrate the denatured slides using an ice-cold ethanol series (80%, 90% and absolute).
7. Incubate the cells with FISH probes at 42 °C under dark and humid conditions overnight (16 h).

Washing and counterstaining

8. Wash hybridized slides with 50% formamide/2× SSC and 2× SSC at 45 °C to remove unbound probes.
9. Label stained slides with DAPI.

? TROUBLESHOOTING

Furthermore, these nucleotides may be transcribed and translated into proteins to understand how cancer cells interact and manipulate their microenvironments directly or via bioinformatic tools (e.g., the European Molecular Biology Laboratory (EMBL) Nucleotide Sequence Database). Finally, the information can complement findings in cell-free genetic studies[71].

There are three distinct features of the spiral biochip that make it valuable to clinical and research objectives. First, enumerated CTCs are in suspension and not immobilized on chips, facilitating immediate downstream manipulation and analysis such as culture. Second, the mode of CTC isolation is tumor antigen–independent. Therefore, the platform may potentially be more sensitive than competing immuno-based platforms. In addition, CTC clusters, which are believed to be involved in tumor metastasis, can be retrieved from blood samples[48,72]. Third, we demonstrate high purity in the enriched samples, with WBC depletion of up to 4 log (refs. 39,62). The high specificity in our CTC isolation technique enables greater accuracy during genome sequencing and mapping, as well as single-cell analysis.

Limitations

Although spiral microfluidics eliminates the use of immunoaffinity markers that can have poor sensitivity and specificity, this method currently cannot isolate CTCs below the size of 12 µm. Although CTCs with a size ≥12 µm have been isolated using the spiral chip because of their reduced deformability compared with the normal blood cells, some CTC (<12 µm) loss is expected. Nonetheless, the high isolation efficiency, as determined by various cell lines, can still provide a large pool of CTCs for clinical and research objectives.

In the operation of the spiral chip, sheath fluid is used to influence particle focusing. This creates a larger collection volume that requires additional steps in order to concentrate the CTCs. This problem was eradicated with the generation of a spiral biochip with trapezoidal channels that operates without sheath fluid and at a much higher throughput (1.7 ml per min)[39]. However, the trapezoidal biochip is incapable of removing platelets and RBC debris causing undesirable contamination of enriched CTCs. Nonetheless, RBC lysis and subsequent dilution are necessary to minimize cellular interactions that affect inertial focusing in microchannels. Our tests have shown that total cell loss due to lysis and centrifugation is <8%. Hence, these steps provide a clear advantage for better CTC enumeration. Despite the presence of residual blood cells, CTCs and WBCs have differences in morphologies and surface protein expressions, allowing them to be clearly differentiated. Efforts are being made to further optimize WBC removal via CD45 immunomagnetic beads that can potentially improve purity.

MATERIALS

REAGENTS

- Photoresist AZ9260 (for photolithography, Microchemicals)
  ! CAUTION Personal protective equipment including nitrile gloves, goggles and protective clothing are required when handling photoresist.
- Photoresist developer (AZ 400K; for photolithography; Microchemicals)
- Isopropyl alcohol (for photolithography) **! CAUTION** Toxicity can occur from ingestion, inhalation or absorption of the substance. Wear protective gloves, a lab coat and goggles when handling this chemical.
- PDMS, Sylgard 184 silicone elastomer kit (Dow Corning, Ellsworth Adhesives, cat. no. 184 Sil Elast kit, 0.5 kg)
- Trichloro (1*H*,2*H*,2*H*,2*H*-perfluorooctyl) silane (for soft lithography, silanizing the surface of newly made silicon master; Sigma-Aldrich, cat. no. 448931-10G) **! CAUTION** Wear protective gloves, a lab coat and goggles when handling this chemical. The silanization process with this chemical should be performed in a chemical hood.
- Polystyrene beads, 9.51 and 20.66 µm (Polysciences, cat. nos. 64120 & 19096)
- Polystyrene beads, 2.02, 4.16, 9.94 and 15.45 µm (Bangs Laboratories)
- Liquid artificial cochineal color (Star brand)
- Sterile PBS, 1× (Corning, cat. no. 21-040-CV)
- BSA, 10% (wt/vol) (Miltenyi Biotec, cat. no. 130-091-376)

- High-glucose DMEM (Life Technologies, cat. no. 11965-092)
- FBS (Life Technologies, cat. no. 10313-039)
- Penicillin-streptomycin (Life Technologies, cat. no. 15140-122)
- Mili-Q purified water
- Trypsin, 0.25% (wt/vol) with EDTA (Lonza, cat. no. CC-5012)
- Cells of interest, e.g., MCF-10, MDA-MB-231, A549 (ATCC, cat. no. HTB-22, CRM-HTB-26, CCL-185) ! CAUTION The cell lines used in your research should be regularly checked to ensure that they are authentic and not infected with mycoplasma.
- RBC lysis buffer, 3× (G-Bioscience, cat. no. 786650)
- Fresh blood sample drawn into an EDTA Vacutainer tube (BD Vacutainer, cat. no. 366643) ! CAUTION Treat all blood as potentially infectious. Wear protective gloves and a lab coat when handling blood. Dispose of contaminated waste according to regulations. Obtain the relevant immunization against blood-borne diseases including Hepatitis B and Tetanus. ! CAUTION Informed consent must be obtained before blood collection from human subjects. Collection must conform to all relevant governmental and institutional regulations. ▲ CRITICAL All blood samples must be processed within 2–4 h after collection.
- Fixative for counting of CTCs consisting of paraformaldehyde (Sigma-Aldrich, cat. no. P6148) ! CAUTION This substance is a suspected carcinogen. Wear protective gloves, a lab coat and goggles when handling this chemical.
- Appropriate conjugated antibodies. We use fluorescein isothiocyanate (FITC)-conjugated pan-cytokeratin (pan-CK) antibody (1:100; Miltenyi Biotec Asia Pacific) and allophycocyanin (APC)-conjugated CD45 antibody (1:100); Miltenyi Biotec Asia Pacific) for identifying putative CTCs. These antibodies can be stored at 4 °C until the expiration date, as indicated on the vial label.
- 0.1% (vol/vol) Triton X-100 (Thermo Scientific, cat. no. 85111) ! CAUTION Wear protective gloves, a lab coat and goggles when handling this chemical.
- Hoechst dye (Life Technologies, cat. no. 33342), if nuclei staining is required
- Fixative for DNA-FISH, consisting of acetic acid and methanol (1:3, both Sigma-Aldrich)
- RNase (4 mg/ml; Sigma-Aldrich, cat. no. R6418)
- Tween 20 (Sigma-Aldrich)
- 70% (vol/vol) formamide/2× SCC (Sigma-Aldrich) for 10 min at 80 °C ! CAUTION Toxicity can occur from ingestion, inhalation or absorption of formamide. Wear protective gloves, a lab coat and goggles when handling this chemical.
- FISH probes (Abbott, cat. no. 02J01)
- 50% formamide/2× saline sodium citrate (PathVysion, Abbott)
- 2× saline sodium citrate (SSC)
- DAPI (Vector Laboratories)

EQUIPMENT

- Silicon wafer, 6 inch (for photolithography)
- UV mask aligner (for photolithography; SUSS MicroTec)
- Spin coater (for photolithography; Dong Ah Trade)
- Photo mask (for photolithography, spiral feature printed on transparent film) printed by Infinite Graphics Incorporated, Singapore. UV exposure of the master is carried out according to MicroChemical's protocol (e.g., 1,700 mJ/cm^2, 180 s for a 12-µm-thick film)
- Deep reactive ion etcher machine (STS, LpX Pegasus)
- Nitrogen gas (for photolithography, dust particle removal from silicon wafer)
- Hot plates (for photolithography and soft lithography, baking photoresist films and PDMS device; DongSeo Scientific)
- Vacuum desiccator (for soft lithography, PDMS solution degassing, GAST)
- Wooden ice-cream sticks for PDMS mixing
- Oven (for curing PDMS molds)
- Sharp tweezers
- Scotch tape (Scotch Magic Tape)
- Disposable biopsy puncher with a plunger system, 1.5-, 2- and 4-mm diameter (Integra Miltex, cat. no. 33-31A-P/25, 33-31-P/25, 33-34-P/25)
- Glass slide, 76 mm × 52 mm (VWR, cat. no. 48312-018)
- Oxygen plasma cleaner (Covance, Femto Science)
- Retort stand
- Inverted phase contrast microscope (Olympus, IX71 & IX81)
- High-speed camera (VisionResearch, Phantom v9)
- 12-bit electron multiplying charged-coupled device (EM-CCD) camera (Andor Technology, iXon+885)
- Computer installed with ImageJ (NIH) and MetaMorph (Molecular Devices) software
- Precision syringe tips (Nordson EFD, cat. no. 7018302)
- Syringe pumps (Harvard apparatus, cat. no. 703006INT; Chemyx, model fusion 200)
- Silicone tubing, inner diameter (i.d.) 0.020 inch, outer diameter (o.d.) 0.060 inch (Tygon, cat. no. AAQ04103)
- Conical tubes, 15 ml and 50 ml (BD Falcon, cat. nos. 352096 & 352070)
- Disposable syringes, 10 ml and 60 ml (Terumo, cat. nos. SS-10ES & BS-60ES)
- Nalgene filter system, 500 ml (Thermo Scientific, cat. no. 566-020)
- Microscope slide (CLP, cat. no. 7105)
- Cover slide (Fisher Scientific, cat. no. 12-545-100)
- Incubator at 37 °C, 5% CO_2 (Thermo Scientific)
- Water bath at 37 °C (Fisher Scientific)
- Biosafety cabinet
- Cell counter (Biorad, TC20)
- Cell culture flask, T25 (BD Biosciences, cat. no. 353108)
- Cell culture dish (Thermo Scientific, cat. no. 168381)
- 96-well plates (Sigma-Aldrich, cat. no. 3596)
- Timer (Fisher, cat. no. S407992)
- Flow cytometer (BD Biosciences, LSR II & Accuri C6)
- Cytospin centrifuge (Thermo Scientific, A78300003)

REAGENT SETUP

Complete DMEM Complete DMEM is DMEM supplemented with 10% (vol/vol) FBS and 1% (vol/vol) penicillin-streptomycin. This solution is stable for several weeks at 4 °C.

Priming solution Priming solution is 1× PBS and 2 mM EDTA supplemented with 0.5% (wt/vol) BSA. This solution is stable for several months at 4 °C.

Blood samples spiked with cell lines To create a blood sample with a low number of cancer cells, dilute the cell suspension to ~1 × 10^5 cells per ml. Add 10 µl of the diluted cell stock to a hemocytometer slide and image it. Manually count the cells to obtain an accurate count, and then transfer the corresponding volume from the diluted cell stock to blood. ▲ CRITICAL This sample can be used to evaluate assay efficiency.

PROCEDURE

Design and mold preparation for spiral biochips ● TIMING 5–7 d

1| Draw the microfluidic design in the AutoCAD software (**Fig. 3a**). The specific design used for fabrication of spiral biochips is available as **Supplementary Data 1**.

2| Submit the design (normally as an AutoCAD file) to a vendor for mask printing. We usually receive the mask in 5–7 business days. Alternatively, the master mold can be made using conventional micromilling on aluminum or stainless steel. The advantage of this approach is that the master mold for biochip replication does not require silanization, and it can be reused for extended periods. **Supplementary Figure 2** shows an optical picture of such a mold.

Master fabrication for spiral biochip (photolithography) ● TIMING 7–10 h

▲ CRITICAL Steps 3–9 must be performed in a clean room.

3| Dispense ~6 ml of AZ9260 photoresist onto a cleaned and dehydrated 4-inch wafer.

4| Spin-coat the dispensed AZ9260 film uniformly on the wafer using a spinner by first ramping to 500 r.p.m. at 100 r.p.m./s acceleration for 10 s and then ramping to 3,000 r.p.m. at 500 r.p.m./s acceleration for 30 s.

5| Prebake the coated wafer for 5 min at 110 °C.
▲ **CRITICAL STEP** The coated wafer should be level while baking.

6| Use a feature-printed transparent film mask to produce the master by exposing the wafer to an appropriate dose of UV light. The specific design used for fabrication of the film mask is available as **Supplementary Data 1**.

7| Develop the exposed wafer in a photoresist developer (AZ400K) for 5 min (1:4 dilution).

8| Rinse the substrate thoroughly with deionized water, and then dry it with a gentle stream of pressurized nitrogen gas.

9| Use a DRIE machine to etch the silicon wafer for ~165 ± 5 μm. The correct etching depth is crucial for optimum performance of the spiral biochip. If the channel depth is <160 μm or >170 μm, the particle focusing will be compromised, thus causing substantial contamination of the enriched sample.

10| Use a vacuum desiccator to silanize the silicon wafer with 150 μl of trichloro(1*H*,2*H*,2*H*,2*H*-perfluorooctyl)silane for 1.5 h.
■ **PAUSE POINT** The silanized wafer master can be stored under a cover to prevent dust exposure for extended periods, and it can be reused for further device fabrication using soft lithography.

Production of spiral biochips (soft lithography) ● **TIMING 1–2 d**
▲ **CRITICAL** The soft lithography procedure can be performed outside the clean room in the lab environment.
11| Mix PDMS base with PDMS curing agent homogeneously at a weight ratio of 10:1. With the silanized wafer master secured (using a double-sided adhesive) in the center of a 15-cm-diameter Petri dish, pour 77 g of the PDMS mixture into the dish.

12| Degas the PDMS in a vacuum desiccator for ~1h. When the PDMS is bubble-free, bake the dish with master (from Step 10) at 70–80 °C inside the oven for at least 2 h to cure the PDMS.

13| Cut and peel the cured PDMS from the master.
▲ **CRITICAL STEP** Measure the height of the cured PDMS device for the first casting to ensure that the channel heights of the fabricated device are within tolerance—i.e., 1–5 μm.
■ **PAUSE POINT** The cured PDMS can be kept in a clean environment for extended periods.

14| Punch holes to create inlets and outlets of the device at appropriate points for each PDMS piece. For a one-layer spiral chip, use a 1.5-mm-diameter puncher. To enable higher throughput with a multiplexed device with several levels, use a 4-mm-diameter puncher for the bottom layers and use a 1.5-mm-diameter puncher for the topmost layer.

15| Clean all the PDMS surfaces and glass slide with Scotch tape by gentle tapping. Ensure that the entire area is in contact with the tape, and check for any dirt visually.
▲ **CRITICAL STEP** Leaving PDMS adherent to the tape for an extended period may leave adhesive residual on the surface, and it may thus affect bonding to PDMS and glass.

16| Plasma-clean the PDMS pieces with features and the glass slide with surfaces to be bonded facing up. The settings we use for plasma treatment are described in the table below.

Parameter	Value
Etcher model	Convance 2MP
Chamber dimension	140 mm (diameter) × 220 mm (height)
RF frequency	13.56 MHz
RF power	300 W
Pressure	760–10^{-3} Torr
End point	100%
Time	2 min 30 s
Oxygen or air flow rate	2 standard cubic centimeters per min (s.c.c.m.)
Ambient temperature	22 °C
Ambient humidity	22–45%

17| Bond the featured PDMS piece to the glass slide by bringing the bonding faces into contact, and press the device softly for 30 s with a pair of tweezers to complete the bonding.
▲ **CRITICAL STEP** To avoid channel collapse, do not apply pressure on top of the microchannel feature directly. For fabricating the multiplexed device, the bonding is done between two featured PDMS pieces, and caution should be taken for the alignment of inlet and outlet reservoirs of different layers.

18| Place the bonded PDMS device on an 85 °C hot plate or oven for 30 min to further strengthen the bonding. Allow cooling for 5 min.
■ **PAUSE POINT** The bonded PDMS device can be kept in a clean environment until further use.

19| Repeat Steps 11–13 as appropriate to get multiple replicas of the featured PDMS pieces, and then repeat Steps 14–18 to bond the featured pieces together and make the multiplexed device. One can first perform one-to-one bonding to create the assembled pieces with a two-layer structure, and then perform bonding between the assembled pieces to get the final multiplexed device with desired copies of spiral channel.

Chip priming ● TIMING 15–30 min
20| Connect tubing to the inlet and outlets of the microfluidic device.

21| Prime the devices for 10–15 min before running the samples. Use syringe pumps to control the flow rates, and capture flow videos with a microscope and a high-speed camera.
▲ **CRITICAL STEP** Check for any air bubbles or debris that can disturb flows in the microfluidic device. The retort stands should also be at the same height for all experiments to ensure consistency in pressure. **Supplementary Figures 3** and **4** schematically show the CTC isolation setup.
? TROUBLESHOOTING

22| If sterile conditions are desired (for culturing and so on), load 70% (vol/vol) ethanol in sterile deionized water into a syringe, and then remove any visible air bubbles within the syringe by pushing the plunger forward. If you are performing nonsterile experiments, this and Steps 23 and 24 are not necessary.
▲ **CRITICAL STEP** Step 27 can be performed before Steps 22–26 if desired.

23| Connect the loaded syringe to one of the spiral inlets via a precision syringe tip and 1.5-mm-diameter silicone tubing, and then insert separate tubing (i.e., with identical length (~15 cm)) to the outlets of the spiral chip to deliver the output sample in target collection tubes.

24| Mount the syringe on the syringe pump and run the 70% (vol/vol) ethanol to the spiral chip at appropriate flow rate (750 µl/min for a single device) for 5 min to sterilize the system and to get rid of bubbles within the system.

25| Load sheath buffer (1× sterile PBS with 0.5% (wt/vol) BSA) into a separate 60-ml syringe, run the sheath buffer through the system for 5 min to coat the surface of microchannels and wash the residual ethanol from the system.

26| Use the inverted microscope and the bright-field mode to inspect the microfluidic channels and ensure that no air bubbles are trapped in the channels. Increasing the flow rate of sheath buffer may help remove the bubbles.
▲ **CRITICAL STEP** If bubbles cannot be removed, a new chip should be used.
? TROUBLESHOOTING

27| Run a quality control (QC) check with the primed device using a particle suspension (~3–6-µm-diameter particles at 0.1% vol/vol) and sheath buffer. Connect a syringe loaded with particle suspension to the outer inlet of the spiral chip, and connect the syringe loaded with sheath buffer to the inner inlet of the chip. After mounting both syringes onto the pumps, proceed to run the particle suspension at a flow rate of 100 µl/min and sheath buffer at 750 µl/min through the single spiral until the particle suspension is observed to enter the main microchannel.
? TROUBLESHOOTING

Blood preparation ● TIMING 30 min
28| To lyse blood, warm the blood sample to room temperature (24–26 °C) and add 3× RBC lysis buffer at a 1:3 vol/vol ratio. Invert the conical tube to mix, and incubate the mixture for 5 min at room temperature on a shaking platform or with periodic inversions, until the color changes to dark red.
▲ **CRITICAL STEP** If you are using blood spiked with cancer cells, spike in the desired number of cancer cells before RBC lysis, as described in Reagent Setup.

29| After the incubation, collect the cells by centrifugation at 1,000*g* for 5 min at room temperature, and resuspend the cell pellet in 1× PBS to the desired concentration optimized for the protocol (2× concentrated, ~14 × 10^6 nucleated cells per ml).

30| Mix it well to resuspend the pellet by tapping the tube gently or by mild pipetting.

31| Place the sample on ice.
■ **PAUSE POINT** Lysed blood samples can be stored for 2–4 h at 4 °C until processing.

Processing lysed blood using a single or multiplexed spiral biochip ● TIMING 10–30 min
32| Adjust the microscope lens (10× magnification) to see the spiral outlet.

33| Place the sterile 15-ml (for enriched sample collection) and 50-ml (for waste collection) conical tubes at the waste and sample outlet collection point.

34| Connect the 50-ml syringe filled with running buffer to the sheath inlet of the spiral chip. The flow rate of this pump should be set to 750 µl/min for processing using a single spiral, or to 2,100 µl/min for processing using the multiplexed chip (three spirals).

35| Prime the biochip by running the sheath buffer at the present flow rate of 750 µl/min for ~2 min.

36| Load the sample syringe containing lysed sample with desired concentration into the second pump, and then adjust the flow rate to 100 µl/min. Connect the syringe to the chip using Tygon tubing and a precision tip.
▲ **CRITICAL STEP** Extra care should be taken for this step to ensure that the syringe plunge is not being pushed excessively and spilling the sample.

37| Processing of the sample begins by flowing in the sheath buffer for ~1 min, until the flow stabilizes. After stabilization, guide the sample collection tubing into the 15-ml conical tube, start the sample pump and continue the collection for ~10–30 min (for 7.5 ml of lysed blood).
▲ **CRITICAL STEP** The processing must be allowed to be completed without disturbing the setup.
? TROUBLESHOOTING

Immunofluorescence staining on isolated cells ● TIMING 30–60 min
▲ **CRITICAL** Cells need to be stained before counting of CTCs.
▲ **CRITICAL** As an alternative to immunofluorescence staining, cells can be characterized by FISH (see **Box 1**).
38| Concentrate the samples collected in Step 37 by centrifuging at 300*g* for 3 min at room temperature.

39| Remove excess supernatant and resuspend the cells in ~250 µl of PBS.

40| Fix the cells with 4% (wt/vol) paraformaldehyde for 10 min at room temperature.
! CAUTION This substance is a suspected carcinogen. Wear protective gloves, a lab coat and goggles when you are handling this chemical.

41| Wash the fixed cells with 1–2 ml of PBS buffer supplemented with 0.5% (wt/vol) BSA, and then centrifuge the mixture at 300*g* for 3 min at room temperature.
■ **PAUSE POINT** Fixed cells can be stored overnight in PBS buffer at 4 °C.

42| Remove excess supernatant and resuspend the cells in ~250 µl containing 0.1% (vol/vol) Triton X-100 to permeabilize the cells for 1–5 min at room temperature.

43| Wash the permeabilized cells with 1–2 ml of PBS buffer supplemented with 0.5% (wt/vol) BSA, and centrifuge it at 300*g* for 3 min at room temperature.

44| Add the required conjugated antibodies directly to the cell suspension, and then incubate it on ice for 30 min. We use conjugated antibodies such as FITC-conjugated pan-cytokeratin (CK) antibody (1:100) and APC-conjugated CD45 antibody (1:100) for identifying putative CTCs. We also add Hoechst dye (1 M, 1:1,000) to the staining solution for nuclei staining.

45| Wash stained cells with 1–2 ml of PBS buffer supplemented with 0.5% (wt/vol) BSA, and then centrifuge the mixture at 300*g* for 3 min at room temperature.

46| Resuspend the stained cells into ~250 µl and transfer them to a single well of a 96-well plate.
■ **PAUSE POINT** Stained cells can be stored overnight in PBS buffer under dark conditions at 4 °C.

Counting or characterization of cells ● TIMING variable

47| Count the cells using a custom-made imaging platform (option A) or manually (option B).

(A) Imaging and CTC enumeration using a custom-made platform ● TIMING 45 min (per well)

(i) Image and scan each well. We use an Olympus inverted microscope (emission filters ET460/50m, ET535/50m and ET 605/70), which has an automated stage. Each well is scanned in a 1 mm × 1 mm grid format using the Metamorph software. For thorough mapping and enumeration of cells in a single well, we select the manual threshold function in the ImageJ software to select for particles corresponding to desired selection.

(B) Manual counting of cells

(i) Obtain images of cells at 40× magnification.

(ii) Compare the corresponding image sets. We identify Hoechst-positive/pan-CK$^+$/CD45-negative (CD45$^-$) cells with round nuclei and high nuclear-to-cytoplasmic (N/C) ratio. These cells are considered to be putative CTCs and their ratio compared with other cell types is determined.

? TROUBLESHOOTING

? TROUBLESHOOTING

Troubleshooting advice can be found in **Table 1**.

TABLE 1 | Troubleshooting table.

Step	Problem	Possible reason	Solution
21	Residual PDMS is trapped in the spiral channel	PDMS is trapped during the punching process	Increase the flow rate of the sheath buffer or replace the chip with a new one
26	Air bubbles are trapped in the spiral channel	Bubbles in the buffer or sample	Increase the flow rate of the sheath buffer or replace the chip with a new one
27	Incorrect particle and cell focusing	Incorrect channel height (i.e., it must be 165–170 µm), which can be the result of improper DRIE	A new master mold must be fabricated
37	No stabilization in the outlet	There is a bubble trapped in the middle of channels or incorrect flow rate	Make sure that the entire chip is bubble-free and that all the parameters (flow rate and syringe diameter) are correct
	Clogging	Large clusters are trapped in the bifurcation point	Stop the enrichment process, and clean the chip by increasing the flow rate of the sheath flow or by replacing with a new chip
47	False positives	Insufficient blocking, expired antibody reagents, inappropriate antibody concentration	Increase BSA concentration to at least 2%, and reduce the antibody concentration to 1:150. Use fresh antibodies
Box 1	High background	Unspecific signals because of nonoptimal probe concentration or insufficient washing	Reduce the probe concentration. Increase the wash buffer volume and washing time
	No signals detected	Insufficient permeabilization or inappropriate fixation	PFA should not be used for fixation. Fresh acetic acid/methanol fixative should be prepared for use

● TIMING

Reagent setup, preparation of blood sample spiked with cell lines for evaluation of assay efficiency: 60 min
Steps 1 and 2, design and mold preparation for spiral biochips: 5–7 d
Steps 3–10, master fabrication for spiral biochip (photolithography): 7–10 h
Steps 11–19, production of spiral biochips (soft lithography): 1–2 d
Steps 20–27, chip priming: 15–30 min
Steps 28–31, blood preparation: 30 min

Steps 32–37, processing lysed blood using a single or multiplexed spiral biochip: 10–30 min
Steps 38–46, immunofluorescence staining on isolated cells: 30–60 min
Step 47, counting or characterization of cells: variable; 45 min–2 d
Box 1, DNA-FISH: 2 d

ANTICIPATED RESULTS

This protocol describes how to perform a high-throughput method of CTC enrichment under high sensitivity and purity. As an example of the results that can be obtained, we show characterization of the system using cell lines (see INTRODUCTION), and processed clinical blood samples from patients with locally advanced or metastatic non-small-cell lung cancer (n = 15) or breast cancer (n =15). Enriched cells were stained with pan-CK (epithelial markers consisting of CK8, CK9, CK18 and CK19) and CD45 (leukocyte marker) antibodies to validate the presence of epithelial cancer cells (**Fig. 5a**). Pan-CK$^+$/CD45$^-$/Hoechst$^+$ round cells with a high nuclear-to-cytoplasmic ratio were enumerated as putative CTCs. These parameters have been adopted from those used in disseminated tumor cell identification[73]. We converted the cell count to CTCs/ml for comparative analysis between samples. Further immunostaining with ET-associated markers revealed varied expression in putative CTCs for EpCAM, CD44, CD24 and E-cadherin (**Fig. 5b–d**). Strikingly, the protocol was able to identify CD44$^+$CD24$^-$Hoechst$^+$ cells, corresponding to the subpopulation of breast cancer stem cells[74]. Cancer stem cells are known to be tumorigenic and to display tolerance or resistance to certain drug therapies[75].

As a negative control, we processed 10 samples from healthy volunteers, and we derived a threshold of >7 CK$^+$ cells for positive patient samples (**Fig. 6a** and **Supplementary Table 3**). We were able to isolate a range of 12–1,275 CK$^+$ breast CTCs and 10–1,535 CK$^+$ lung CTCs from patient samples, which were clearly distinguished from those obtained from healthy samples. The label-free technique is also able to isolate CTC clusters (microemboli) (**Fig. 6b**, top left), an observation that has been reported to correlate with improved survival and proliferation[76]. CTCs enriched from samples obtained from patients either with lung cancer or breast cancer were labeled positive for a rare *ALK* (encoding anaplastic lymphoma receptor tyrosine kinase) mutation with the *ALK* break-apart probe using DNA-FISH (**Fig. 6b**, bottom left) or HER2/neu amplification using DNA-FISH, respectively (**Fig. 6b**, bottom right). In addition, enriched CTCs are viable, potentially allowing downstream assays including culture (**Fig. 6b**, top right)[50]. There are currently ongoing efforts to further purify the CTC fraction and improve the current yield of our spiral device for use in delicate downstream analysis, such as sequencing (**Fig. 6c**).

If the microfluidics devices are fabricated and primed as described, the spiral biochips are easy to use and can be further manipulated according to specific needs. The reported data were obtained by graduate students

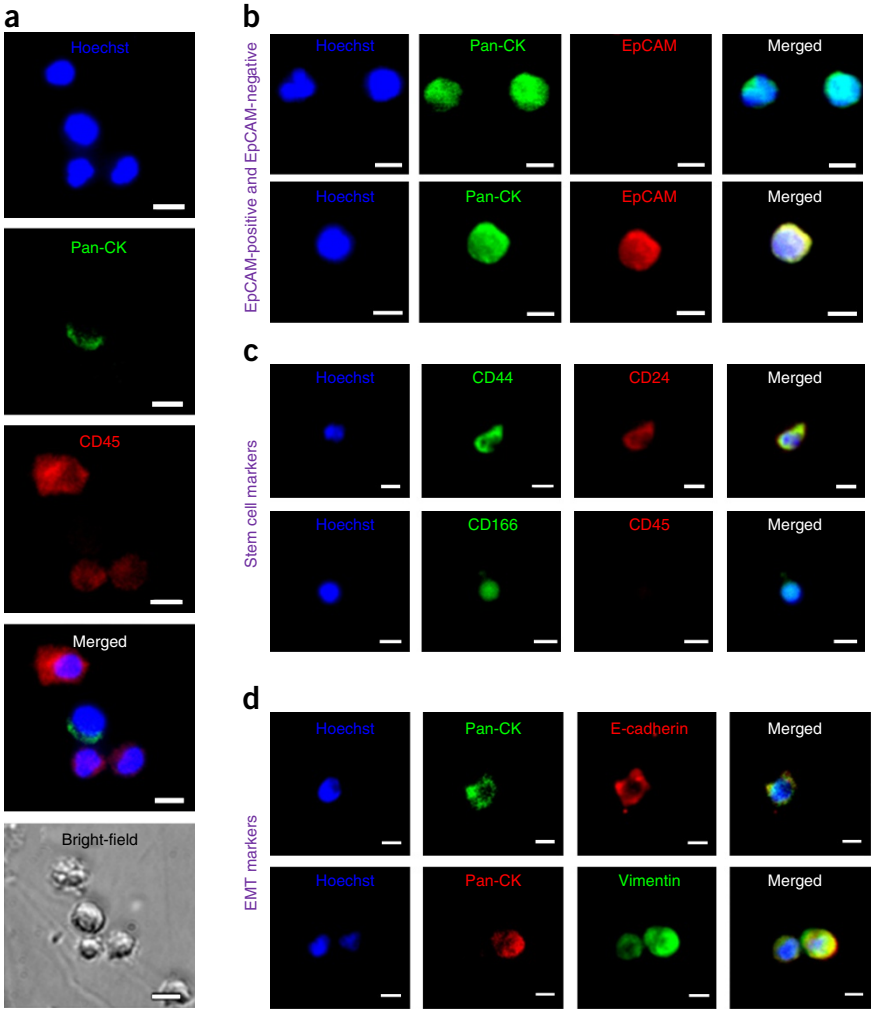

Figure 5 | Immunostaining of enriched CTCs from clinical patient blood samples. (**a**) Enriched cells were stained with pan-CK (epithelial marker) and CD45 (leukocyte marker) antibodies (1:100, Miltenyi Biotec Asia Pacific) to validate the presence of epithelial cancer cells. Enriched cells were also stained with a variety of EMT-associated markers, such as EpCAM (**b**), CD44, CD24 (**c**) and E-cadherin (**d**), to illustrate the heterogeneity of the CTCs isolated with a label-free technique. Informed consent was obtained before blood collection from human subjects. Scale bars, 20 μm.

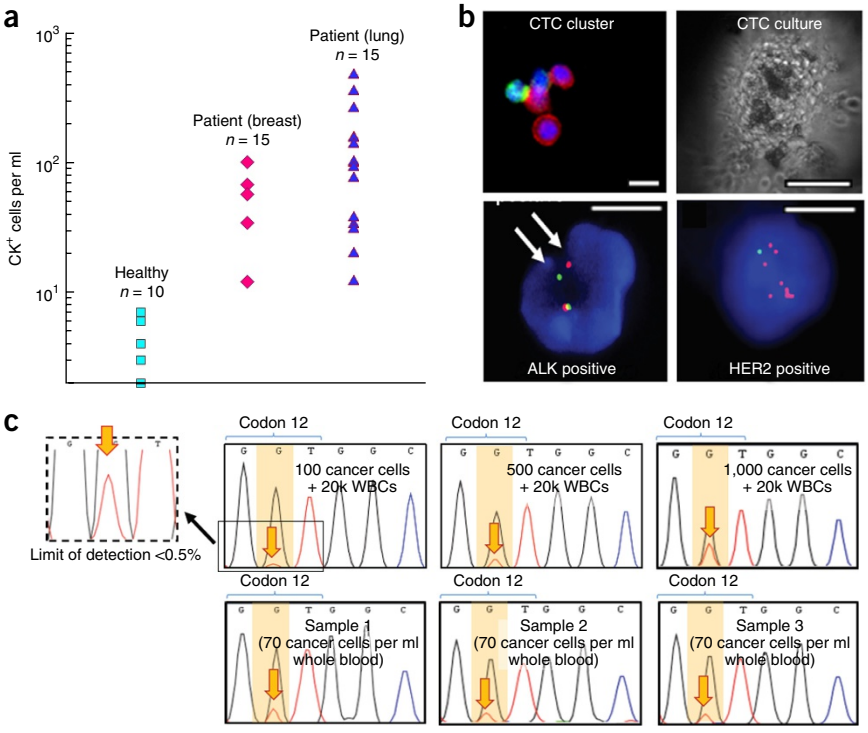

Figure 6 | Validation of the spiral inertial biochip for clinical analysis. (**a**) pan-CK$^+$CD45$^-$Hoechst$^+$ (pan-CK– and CD45–specific antibodies from Miltenyi Biotec Asia Pacific; Hoechst from Life Technologies) cells that were round cells with high nuclear-to-cytoplasmic ratio were enumerated as putative CTCs. These cell counts were expressed as CTCs/ml for convenience in comparison between samples. As a negative control, ten samples from healthy volunteers were also processed, enabling us to obtain a threshold of >7 CK$^+$ cells for positive patient samples. A range of 12–1,275 CK$^+$ breast CTCs and 10–1,535 CK$^+$ lung CTCs were obtained from these patient samples, which is clearly distinguished from those obtained with healthy samples. (**b**) Top left, image of microemboli isolated from the microfluidics biochips. Scale bar, 20 µm. Bottom left, CTCs enriched from a sample obtained from a particular patient with lung cancer were labeled as positive for a rare *ALK* mutation with the *ALK* break-apart probe using DNA-FISH. Scale bar, 20 µm. Bottom right, CTCs enriched from a sample obtained from a particular patient with breast cancer were labeled as positive with HER2/neu amplification using DNA-FISH. Scale bar, 20 µm. Top right, enriched CTCs are viable, allowing downstream assays including culture. Scale bar, 100 µm. (**c**) Sequencing results for *KRAS* codon 12 mutation. ICE-COLD (Improved and Complete Enrichment CO-amplification at Lower Denaturation temperature) PCR was performed, followed by Sanger sequencing. *KRAS* mutation was detected by base calling. Top row, controls using known number of spiked SW480 cells in 20,000 WBCs were used to determine the detection limit. Bottom row, mutational analysis of DNA in enriched sample from spiral biochip shows markedly higher signal than the detection limit. Informed consent was obtained before blood collection from human subjects.

and post-doctorates in the laboratory, but the device has since been used in several other laboratories by people with little experience in spiral microfluidics. Adequate initial guidance for about three runs should be sufficient to enable operators to carry out the protocol independently, based on our experience. Problems in fully executing the protocol generally only arise if there are errors in mold fabrication or sample quality (clogs and so on; see **Table 1**).

Note: Any Supplementary Information and Source Data files are available in the online version of the paper.

ACKNOWLEDGMENTS We express our sincere gratitude to all patients and healthy volunteers who participated in this trial and donated blood samples for characterization of our device. Financial support by the Singapore-MIT Alliance for Research and Technology (SMART) Center (BioSyM IRG) is gratefully acknowledged. This work is also supported by the use of NTU's Micro-Machine Center (MMC) facilities for wafer fabrication and the lab facilities at the Mechanobiology Institute (MBI) and the Nano Biomechanics Laboratory at the National University of Singapore. The clinical sample and data collection was supported by the Singapore National Medical Research Council grant no. NMRC 1225/2009.

AUTHOR CONTRIBUTIONS M.E.W., B.L.K., L.W., A.K.P.T., A.A.S.B. and C.T.L. contributed to the design of the spiral biochips. M.E.W., B.L.K., L.W., A.K.P.T. and A.A.S.B. prepared the manuscript and J.H. and C.T.L. commented on the manuscript.

COMPETING FINANCIAL INTERESTS The authors declare competing financial interests: details are available in the online version of the paper.

1. Jemal, A. *et al.* Global cancer statistics. *CA Cancer J. Clin.* **61**, 69–90 (2011).
2. Esmaeilsabzali, H., Beischlag, T.V., Cox, M.E., Parameswaran, A.M. & Park, E.J. Detection and isolation of circulating tumor cells: principles and methods. *Biotechnol. Adv.* **31**, 1063–1084 (2013).
3. Gupta, G.P. & Massagué, J. Cancer metastasis: building a framework. *Cell* **127**, 679–695 (2006).
4. van de Stolpe, A., Pantel, K., Sleijfer, S., Terstappen, L.W. & den Toonder, J.M. Circulating tumor cell isolation and diagnostics: toward routine clinical use. *Cancer Res.* **71**, 5955–5960 (2011).
5. Ashworth, T. A case of cancer in which cells similar to those in the tumours were seen in the blood after death. *Australian Med. J.* **14**, 146–149 (1869).
6. Wittekind, C. & Neid, M. Cancer invasion and metastasis. *Oncology* **69**, 14–16 (2005).
7. Racila, E. *et al.* Detection and characterization of carcinoma cells in the blood. *Proc. Natl. Acad. Sci.* **95**, 4589–4594 (1998).
8. Adalsteinsson, V.A. & Love, J.C. Toward engineered processes for sequencing-based analysis of single circulating tumor cells. *Curr. Opin. Chem. Eng.* **4**, 97–104 (2014).
9. Majid, E.W. & Lim, C.T. *Microfluidic Platforms for Human Disease Cell Mechanics Studies* (Springer, 2013).
10. Lara, O., Tong, X., Zborowski, M. & Chalmers, J.J. Enrichment of rare cancer cells through depletion of normal cells using density and flow-through, immunomagnetic cell separation. *Exp. Hematol.* **32**, 891–904 (2004).
11. De Giorgi, V. *et al.* Application of a filtration-and isolation-by-size technique for the detection of circulating tumor cells in cutaneous melanoma. *J. Invest. Dermatol.* **130**, 2440–2447 (2010).
12. Warkiani, M.E. *et al.* Isoporous micro/nanoengineered membranes. *ACS Nano* **7**, 1882–1904 (2013).
13. Matas, J.-P., Morris, J.F. & Guazzelli, E. Inertial migration of rigid spherical particles in Poiseuille flow. *J. Fluid Mech.* **515**, 171–195 (2004).
14. Whitesides, G.M. The origins and the future of microfluidics. *Nature* **442**, 368–373 (2006).

15. Schwartz, M. Molecular characterization of CTCs. *Genet. Eng. Biotechnol. News* **33**, 36–37 (2013).
16. Nagrath, S. *et al.* Isolation of rare circulating tumor cells in cancer patients by microchip technology. *Nature* **450**, 1235–1239 (2007).
17. Gleghorn, J.P. *et al.* Capture of circulating tumor cells from whole blood of prostate cancer patients using geometrically enhanced differential immunocapture (GEDI) and a prostate-specific antibody. *Lab Chip* **10**, 27–29 (2010).
18. Chen, W. *et al.* Nanoroughened surfaces for efficient capture of circulating tumor cells without using capture antibodies. *ACS Nano* **7**, 566–575 (2012).
19. Wang, S. *et al.* Highly efficient capture of circulating tumor cells by using nanostructured silicon substrates with integrated chaotic micromixers. *Angew. Chem. Int. Ed. Engl.* **50**, 3084–3088 (2011).
20. Allan, A.L. & Keeney, M. Circulating tumor cell analysis: technical and statistical considerations for application to the clinic. *J. Oncol.* **2010**, 426218 (2010).
21. Thiery, J.P. & Lim, C.T. Tumor dissemination: an EMT affair. *Cancer Cell* **23**, 272–273 (2013).
22. Prang, N. *et al.* Cellular and complement-dependent cytotoxicity of EpCAM-specific monoclonal antibody MT201 against breast cancer cell lines. *Br. J. cancer* **92**, 342–349 (2005).
23. Maheswaran, S. *et al.* Detection of mutations in EGFR in circulating lung-cancer cells. *N. Engl. J. Med.* **359**, 366–377 (2008).
24. Riethdorf, S. *et al.* Detection and HER2 expression of circulating tumor cells: prospective monitoring in breast cancer patients treated in the neoadjuvant GeparQuattro trial. *Clin. Cancer Res.* **16**, 2634–2645 (2010).
25. Lacroix, M. Significance, detection and markers of disseminated breast cancer cells. *Endocr. Relat. Cancer* **13**, 1033–1067 (2006).
26. Kemmner, W. Currently used markers for CTC isolation-advantages, limitations and impact on cancer prognosis. *J. Clin. Exp. Pathol.* **1**, 102 (2011).
27. Pecot, C.V. *et al.* A novel platform for detection of CK^+ and CK CTCs. *Cancer Discov.* **1**, 580–586 (2011).
28. Sieuwerts, A.M. *et al.* Anti-epithelial cell adhesion molecule antibodies and the detection of circulating normal-like breast tumor cells. *J. Natl. Cancer Inst.* **101**, 61–66 (2009).
29. Fehm, T. *et al.* Methods for isolating circulating epithelial cells and criteria for their classification as carcinoma cells. *Cytotherapy* **7**, 171–185 (2005).
30. Pachmann, K. *et al.* Standardized quantification of circulating peripheral tumor cells from lung and breast cancer. *Clin. Chem. Lab. Med.* **43**, 617–627 (2005).
31. Tkaczuk, K.H.R. *et al.* The significance of circulating epithelial cells in breast cancer patients by a novel negative selection method. *Breast Cancer Res. Treat.* **111**, 355–364 (2008).
32. Alix-Panabières, C. *et al.* Detection of circulating prostate-specific antigen–secreting cells in prostate cancer patients. *Clin. Chem.* **51**, 1538–1541 (2005).
33. Ozkumur, E. *et al.* Inertial focusing for tumor antigen–dependent and–independent sorting of rare circulating tumor cells. *Sci. Transl. Med.* **5**, 179ra47 (2013).
34. Yang, L. *et al.* Optimization of an enrichment process for circulating tumor cells from the blood of head and neck cancer patients through depletion of normal cells. *Biotechnol. Bioeng.* **102**, 521–534 (2009).
35. Munz, M. *et al.* Side-by-side analysis of five clinically tested anti-EpCAM monoclonal antibodies. *Cancer Cell Int.* **10**, 44 (2010).
36. Chaudhuri, P.K., Ebrahimi Warkiani, E., Jing, T., Kenry & Lim, C.T. Microfluidics for research and applications in oncology. *Analyst* http://dx.doi.org/10.1039/C5AN00382B (2015).
37. Hyun, K.A., Kwon, K., Han, H., Kim, S.I. & Jung, H.I. Microfluidic flow fractionation device for label-free isolation of circulating tumor cells (CTCs) from breast cancer patients. *Biosens. Bioelectron.* **40**, 206–212 (2013).
38. Tan, S.J. *et al.* Versatile label free biochip for the detection of circulating tumor cells from peripheral blood in cancer patients. *Biosens. Bioelectron.* **26**, 1701–1705 (2010).
39. Warkiani, M.E. *et al.* Slanted spiral microfluidics for the ultra-fast, label-free isolation of circulating tumor cells. *Lab Chip* **14**, 128–137 (2014).
40. Gertler, R. *et al.* Detection of circulating tumor cells in blood using an optimized density gradient centrifugation. *Recent Results Cancer Res.* **162**, 149–155 (2003).
41. Hur, S.C., Henderson-MacLennan, N.K., McCabe, E.R. & Di Carlo, D. Deformability-based cell classification and enrichment using inertial microfluidics. *Lab Chip* **11**, 912–920 (2011).
42. Moon, H.S. *et al.* Continuous separation of breast cancer cells from blood samples using multi-orifice flow fractionation (MOFF) and dielectrophoresis (DEP). *Lab Chip* **11**, 1118–1125 (2011).
43. Huang, S.B. *et al.* High-purity and label-free isolation of circulating tumor cells (CTCs) in a microfluidic platform by using optically-induced-dielectrophoretic (ODEP) force. *Lab Chip* **13**, 1371–1383 (2013).
44. Cima, I. *et al.* Label-free isolation of circulating tumor cells in microfluidic devices: current research and perspectives. *Biomicrofluidics* **7**, 011810 (2013).
45. Gao, D. *et al.* Organoid cultures derived from patients with advanced prostate cancer. *Cell* **159**, 176–187 (2014).
46. Sollier, E. *et al.* Size-selective collection of circulating tumor cells using Vortex technology. *Lab Chip* **14**, 63–77 (2014).
47. Karabacak, N.M. *et al.* Microfluidic, marker-free isolation of circulating tumor cells from blood samples. *Nat. Protoc.* **9**, 694–710 (2014).
48. Hou, H. *et al.* Isolation and retrieval of circulating tumor cells using centrifugal forces. *Sci. Rep.* **3**, 1259 (2013).
49. Warkiani, M.E. *et al.* An ultra-high-throughput spiral microfluidic biochip for the enrichment of circulating tumor cells. *Analyst* **139**, 3245–3255 (2014).
50. Khoo, B.L. *et al.* Clinical validation of an ultra-high-throughput spiral microfluidics for the detection and enrichment of viable circulating tumor cells. *PLoS ONE* **9**, e99409 (2014).
51. Segre, G. Radial particle displacements in Poiseuille flow of suspensions. *Nature* **189**, 209–210 (1961).
52. Segre, G. & Silberberg, A. Behaviour of macroscopic rigid spheres in Poiseuille flow Part 2. Experimental results and interpretation. *J. Fluid Mech.* **14**, 136–157 (1962).
53. Karnis, A., Goldsmith, H. & Mason, S. The flow of suspensions through tubes: V. Inertial effects. *Can. J. Chem. Eng.* **44**, 181–193 (1966).
54. Tachibana, M. On the behaviour of a sphere in the laminar tube flows. *Rheol. Acta* **12**, 58–69 (1973).
55. Choi, Y.-S., Seo, K.-W. & Lee, S.-J. Lateral and cross-lateral focusing of spherical particles in a square microchannel. *Lab Chip* **11**, 460–465 (2011).
56. Di Carlo, D., Irimia, D., Tompkins, R.G. & Toner, M. Continuous inertial focusing, ordering, and separation of particles in microchannels. *Proc. Natl. Acad. Sci.* **104**, 18892–18897 (2007).
57. Bhagat, A.A.S., Kuntaegowdanahalli, S.S. & Papautsky, I. Continuous particle separation in spiral microchannels using dean flows and differential migration. *Lab Chip* **8**, 1906–1914 (2008).
58. Dean, W. Fluid motion in a curved channel. *Proc. R. Soci. Lond.* **121**, 402–420 (1928).
59. Di Carlo, D. Inertial microfluidics. *Lab Chip* **9**, 3038–3046 (2009).
60. Hayes, D.F. & Smerage, J.B. Circulating tumor cells. *Prog. Mol. Biol. Transl. Sci.* **95**, 95–112 (2009).
61. Kuntaegowdanahalli, S.S., Bhagat, A.A.S., Kumar, G. & Papautsky, I. Inertial microfluidics for continuous particle separation in spiral microchannels. *Lab Chip* **9**, 2973–2980 (2009).
62. Khoo, B. *et al.* Ultra-high throughput enrichment of viable circulating tumor cells. in *The 15th International Conference on Biomedical Engineering (ICBME 2013, 4th* **43**, 1–4 (Springer).
63. Cristofanilli, M. *et al.* Circulating tumor cells: a novel prognostic factor for newly diagnosed metastatic breast cancer. *J. Clin. Oncol.* **23**, 1420–1430 (2005).
64. Smerage, J. & Hayes, D. The measurement and therapeutic implications of circulating tumour cells in breast cancer. *Br. J. Cancer* **94**, 8–12 (2006).
65. Yu, M. *et al.* Circulating breast tumor cells exhibit dynamic changes in epithelial and mesenchymal composition. *Science* **339**, 580–584 (2013).
66. Payne, R. *et al.* Viable circulating tumour cell detection using multiplex RNA *in situ* hybridisation predicts progression-free survival in metastatic breast cancer patients. *Br. J. Cancer* **106**, 1790–1797 (2012).
67. Yu, M. *et al. Ex vivo* culture of circulating breast tumor cells for individualized testing of drug susceptibility. *Science* **345**, 216–220 (2014).
68. Zhang, L. *et al.* The identification and characterization of breast cancer CTCs competent for brain metastasis. *Sci. Transl. Med.* **5**, 180ra148 (2013).
69. Khoo, B.L. *et al.* Short-term expansion of breast circulating cancer cells predicts response to anti-cancer therapy. *Oncotarget* **6**, 15578–15593 (2015).
70. Dittrich, P.S. & Manz, A. Lab-on-a-chip: microfluidics in drug discovery. *Nat. Rev. Drug Discov.* **5**, 210–218 (2006).
71. Wu, T.-L. *et al.* Cell-free DNA: measurement in various carcinomas and establishment of normal reference range. *Clin. Chim. Acta* **321**, 77–87 (2002).
72. Aceto, N. *et al.* Circulating tumor cell clusters are oligoclonal precursors of breast cancer metastasis. *Cell* **158**, 1110–1122 (2014).
73. Borgen, E. *et al.* Standardization of the immunocytochemical detection of cancer cells in BM and blood: I. establishment of objective criteria for the evaluation of immunostained cells. *Cytotherapy* **1**, 377–388 (1999).
74. Al-Hajj, M., Wicha, M.S., Benito-Hernandez, A., Morrison, S.J. & Clarke, M.F. Prospective identification of tumorigenic breast cancer cells. *Proc. Natl. Acad. Sci. USA* **100**, 3983–3988 (2003).
75. Li, X. *et al.* Intrinsic resistance of tumorigenic breast cancer cells to chemotherapy. *J. Natl. Cancer Inst.* **100**, 672–679 (2008).
76. Friedl, P. & Gilmour, D. Collective cell migration in morphogenesis, regeneration and cancer. *Nat. Rev. Mol. Cell Biol.* **10**, 445–457 (2009).